Title
CANCELLED Dichotomous Behavior of Capillary Surfaces in Zero Gravity

Journal
Microgravity Sci. Technol., 3

Authors
Concus, P.
Finn, R.

Publication Date
1990

LBL-29225
Preprint

Lawrence Berkeley Laboratory
UNIVERSITY OF CALIFORNIA

Physics Division

Mathematics Department

To be submitted for publication

Dichotomous Behavior of Capillary Surfaces in Zero Gravity

P. Concus and R. Finn

June 1990

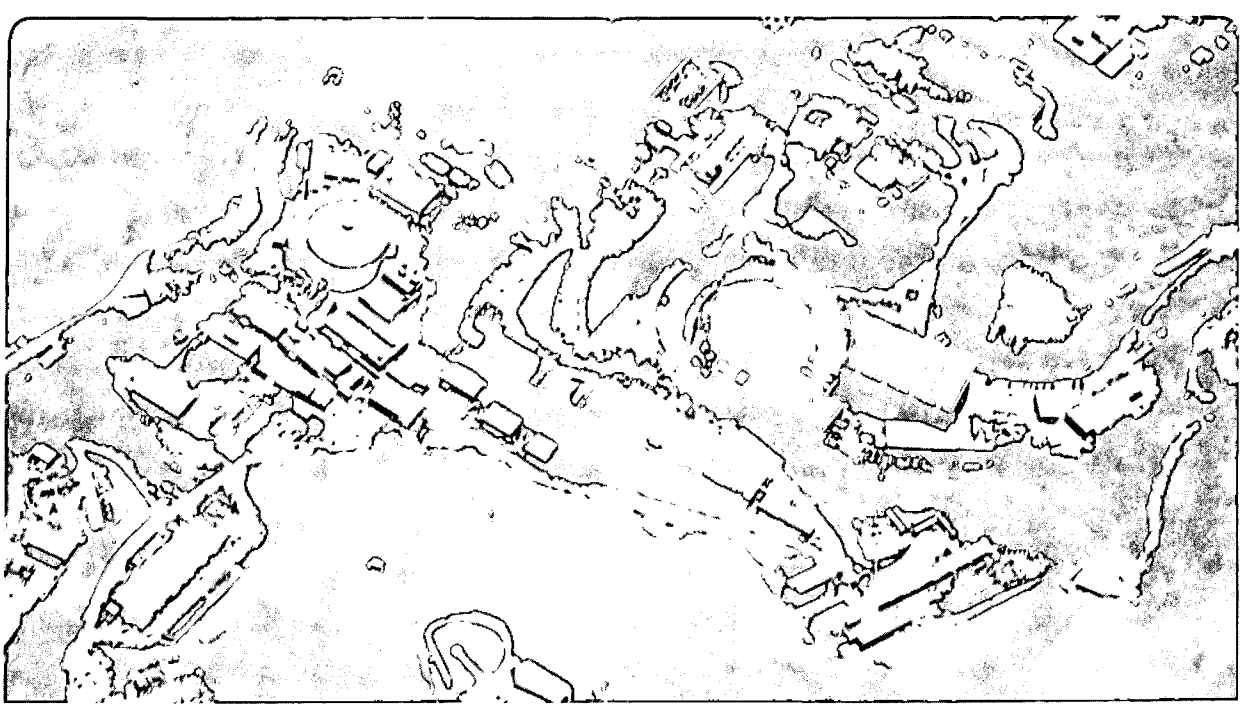

Prepared for the U.S. Department of Energy under Contract Number DE-AC03-76SF00098.

DISCLAIMER

LBL-29225

DICHOTOMOUS BEHAVIOR OF CAPILLARY SURFACES IN ZERO GRAVITY *

Paul Concus
Lawrence Berkeley Laboratory
and
Department of Mathematics
University of California
Berkeley, California 94720

and

Robert Finn
Department of Mathematics
Stanford University
Stanford, California 94305

June 1990

* This work was supported in part by the Applied Mathematical Sciences Subprogram of the Office of Energy Research, U.S. Department of Energy, under Contract Number DE-AC03-76SF000098, by the National Science Foundation, and by the National Aeronautics and Space Administration.

DICHOTOMOUS BEHAVIOR OF CAPILLARY SURFACES IN ZERO GRAVITY

Paul Concus and Robert Finn

Abstract

A mathematical procedure is described for determining the behavior of the free surface of a fluid in static equilibrium and partly filling a cylindrical container with cross-section of general form in zero gravity. Either of two qualitatively distinct situations must prevail, depending on geometry and contact angle. Several illustrative examples are discussed, and the procedure is applied in detail to a container with a rectangular section on which the corners have been rounded, thereby determining the effect of rounding on the "critical" contact angle that separates the two types of behavior. This last example is intended in part as a guide for application to general geometries.

Introduction

The behavior of an equilibrium capillary surface interface can change qualitatively and even dramatically when an external gravity field is allowed to become zero. A striking illustration of this kind of instability can be obtained using cylindrical capillary tubes of non-circular cross-section. Such change in behavior was predicted as a consequence of formal mathematical results established in [2]; the ideas were developed subsequently in, e. g., [6], [7], and Chapter 6 of [8].

In order to include the $g = 0$ case in a unified way, we restrict attention here to tubes closed at the bottom and of infinite height, oriented so that the gravity field, when it exists, is directed vertically downward (see Fig. 1). We refer to this case as $g > 0$. When $g > 0$, then for very general sections Ω—even with quite discontinuous boundary—it can be shown that for sufficiently large prescribed volume V of fluid, there exists a configuration of minimizing mechanical energy for which the free surface interface S lies above and projects simply onto Ω (that is, S is defined by a positive single-valued height $u(x, y; g)$ above the base for every point (x, y) of Ω). In many situations solution surfaces continue to exist when $g = 0$ and are even achievable in the form $u(x, y; 0) = \lim_{g \to 0} u(x, y; g)$. But it can

happen, even when Ω has smooth boundary, that no such surface can be found. When that happens, then regardless of the volume V, every physical configuration must uncover a portion of the base (i.e., fluid moves to the walls). This change in behavior occurs not only for fixed contact angle γ and changing geometry, but it can also happen with a given geometry when γ is varied. For the circular tube—on which attention has classically been focused—the former situation of a simply-projecting free surface S prevails for any γ, and in fact the limiting surface with $g = 0$ is even known explicitly as a spherical cap; that may explain partly the reason that the distinctions in behavior were not observed earlier. The other situation can however be achieved with relatively modest changes of Ω (for example into a suitable ellipse) and thus is important to study.

The predicted dichotomy in behavior for $g = 0$ has been verified experimentally; this was done initially by W. Masica in drop tower experiments, using regular hexagonal cylinders and differing fluids (cf., [2]). A different geometry with less symmetry and without boundary discontinuities (bathtub) was later investigated experimentally by G. Smedley [10], and further evidence for the theoretical predictions was obtained.

Given a geometry and contact angle, no geometrically explicit way is known for predicting which case will occur. However an indirect procedure developed by Finn in a formal mathematical study [7] is effective for many configurations of interest. Because of the precise information yielded by the results and their wide range of applicability, and additionally since descriptions currently available in the engineering literature seem to us deficient in some respects, we offer here an outline of the procedure in a form intended for purposes of engineering design. We emphasize that the results as presented below are mathematically complete and rigorous, granting the underlying hypotheses of classical capillarity theory as introduced by Young, Laplace, and Gauss (see [8, Chapter 1]). Our analysis takes full account of the nonlinearity in the problem, and no simplifying approximations are introduced.

Basic Procedure

In what follows, "existence of a solution" means that for sufficiently large fluid volume an equilibrium physical interface covering the base will be observed. Specifically, there will be a height function $u(x, y)$ satisfying

$$\text{div } Tu = \frac{1}{R_\gamma}, \quad Tu \equiv \frac{\nabla u}{\sqrt{1 + |\nabla u|^2}}$$

in Ω, such that the contact angle condition

$$\nu \cdot Tu = \cos\gamma$$

holds on Σ (see, e. g., [8, Chapter 1]); here Σ is the boundary of Ω, ν is the exterior unit normal on Σ, and

$$R_\gamma = \frac{|\Omega|}{|\Sigma| \cos\gamma}, \tag{1}$$

where $|\Omega|$ and $|\Sigma|$ denote respectively the area and length of Ω and Σ. The amount of fluid actually needed can in many situations be estimated explicitly (see the methods discussed in [8, Chapter 6]; also see [4] for a case of particular interest), but we restrict attention in this article to the more basic question of whether "existence" is in principle possible. We suppose for simplicity that $0 \leq \gamma < \pi/2$ (the complementary case is easily transformed into this one). (For $\gamma = \pi/2$, the solution surface is a horizontal plane for any cross-section.) We introduce circular arcs Γ of radius R_γ lying in Ω and joining two points of Σ; we refer to the "exterior" of Γ as the portion Ω^* of Ω cut off by Γ, that also lies exterior to the circle determined by Γ. We denote by Σ^* the part of the boundary Σ bordering Ω^*. In interpreting the following "basic theorem" reference should be made to Fig 2. We consider first the case in which Σ has continuously turning tangent.

THEOREM (for smooth boundary). *A solution exists for given Ω and γ if and only if, for every subarc Γ of a semicircle of radius R_γ in Ω that meets Σ in angles γ (measured exterior to Γ) , the functional $\Phi(\Omega; \Gamma; \gamma)$ defined by*

$$\Phi \equiv |\Gamma| - |\Sigma^*| \cos\gamma + \frac{1}{R_\gamma}|\Omega^*| \tag{2}$$

is positive.

We refer to an arc Γ that satisfies the conditions indicated in the theorem as an "extremal", for the reason that these arcs arise in the "subsidiary" variational problem of minimizing Φ (see [7] and [8, Chapter 6]; it must be emphasized that in general such arcs are stationary, but need not minimize). The interest of the theorem derives largely from the fact that in most cases of interest only a finite number of extremals (aside from trivial rigid displacements arising from symmetries) can be found in a given domain Ω. Thus the kind of behavior to be expected can in general be predicted with only a finite number of area and length calculations, carried out for particular configurations.

The physical significance of the theorem deserves some comment, which will also be helpful in what follows. It can be shown (cf., [8, p. 144]) that for any Ω, there corresponds an angle γ_{cr}, such that a solution exists when $\gamma_{cr} < \gamma < \pi/2$, while no solution can be found when $0 \leq \gamma < \gamma_{cr}$. We consider a domain Ω for which $0 < \gamma_{cr} < \pi/2$. It is shown in [3] that for $\gamma = \gamma_{cr}$, there will be (at least) one non-null extremal Γ in Ω, with $\Phi(\Omega; \Gamma; \gamma) = 0$. To fix the ideas, we restrict attention at first to those situations in which a single unique such extremal appears. For any $\gamma > \gamma_{cr}$, every extremal Γ will yield $\Phi > 0$, and thus solution surfaces will exist. If we now introduce a family of solutions $u(x, y; \gamma)$ with $\gamma \searrow \gamma_{cr}$, then these solutions can be normalized by additive constants, so that they approach infinity throughout Ω^* and tend to a (bounded) solution surface in $\Omega \backslash \Omega^*$. We note that such solutions cannot be normalized to have constant volume in a container with a bottom, and thus for any given volume V the base will become partly uncovered for some $\gamma > \gamma_{cr}$, depending on V. Because of these striking changes, which in cases of particular interest can be nearly discontinuous, the result lends itself naturally to experimental verification.

The boundary Σ of Ω can be permitted also to have corners, in which case a more general statement of the basic theorem is needed. Let Σ consist of a finite number of smooth arcs, joining at corner points in well defined angles. Such a corner point P is

called *reentrant* if the angle formed interior to Ω at P exceeds π.

THEOREM (General Form). *A solution exists for given Ω and γ if and only if, for every subarc Γ of a semicircle of radius R_γ in Ω such that each intersection point with Σ is either a reentrant corner or else a point interior to a smooth arc of Σ where Γ and Σ meet at angle γ (measured exterior to Γ), the functional $\Phi(\Omega;\Gamma;\gamma)$ defined by*

$$\Phi \equiv |\Gamma| - |\Sigma^*|\cos\gamma + \frac{1}{R_\gamma}|\Omega^*|$$

is positive.

We illustrate the ideas with some examples.

Illustrative Examples

(i) *The circular tube.* One sees readily that when Ω is a circular disk, the extremals are circular arcs that pass through its center, see Fig. 3. There are no extremals unless $\gamma > \pi/4$. Thus, if $\gamma \leq \pi/4$ the conditions of the theorem are vacuously satisfied, and we are assured of the existence of a solution surface. If $\gamma > \pi/4$ nontrivial extremals are present, but a calculation shows that in every such configuration there holds $\Phi > 0$. Thus *the theorem guarantees in every case the existence of a surface interface.* This is of course no surprise, as the case considered is one of the very few in which the solution can be found explicitly. It is a lower spherical cap, of radius chosen to make the prescribed angle with the cylinder walls, and situated in the tube at a height so that it cuts off the prescribed volume V. Note that even in this case if V is too small, there will be no solution covering the base.

(ii) *The bathtub.* In the above example we cut the circular boundary at the endpoints of a diameter, and join the two semicircles by parallel segments of length h, as illustrated in Fig. 4. It is no longer so easy to make the calculations for Φ when extremals exist, however the configuration is a limiting case of the rounded rectangle discussed below, and we obtain as a special case of that discussion that *a solution exists for every γ, regardless*

of h.

This result is remarkable in view of the fact that for an ellipse with ratio of minor to major semiaxes of less than approximately 0.6116, solutions fail to exist when γ is near zero, see [1]. The result is perhaps still more striking in view of the fact that if the straight segments are inclined to one another at an angle α, with smoothly joining end arcs, as in Fig. 5, then for any fixed $\gamma < \pi/2$, an extremal joining the segments and yielding $\Phi \leq 0$ appears and thus solutions will fail to exist, when h is large enough. In fact, *if we fix the (different) radii of the end arcs, then any γ can be excluded by increasing h, even though the segments become progressively closer to the parallel configuration of Fig. 4, for which no γ is excluded.* This nonuniformity in behavior was pointed out and illustrated by calculations in [3]. Further calculations appear in [11], while [10] describes preliminary experimental verification of particular configurations, in a two second drop tower. More recently, experiments on a KC-135 flight with about 15 seconds of free fall have allowed more thorough experimental results, lending convincing support to the theoretical predictions; these experiments will be described in a forthcoming paper [5].

(iii) *The keyhole.* In the example of Fig. 4, we allow the radius R of one of the end caps to increase, keeping the other fixed at a value r, thus obtaining the configuration of Fig. 6. Solutions continue to exist for all γ, regardless of h, until a critical value $R/r \approx 1.974$ is attained. In this configuration, a continuum of extremals Γ corresponding to $\gamma = 0$ appears, joining the parallel sides as indicated in Fig. 6, and all yielding $\Phi = 0$. Although an infinity of essentially distinct extremals appears in this case, nevertheless the behavior described can be ascertained with only a finite number of calculations. If a succession of fluids with contact angles decreasing to zero is inserted into a capillary tube with this section, the volumes can be normalized so that the corresponding solution surfaces will tend to a solution to the right of the extremal arc joining A and B, and will tend uniformly to infinity everywhere to the left of that arc. The domain can be modified so as to cause the "infinity" region to shift, almost discontinuously, from one end of the narrow portion of

the tube to the other, with small changes in contact angle. This leads to a new procedure for measurement of contact angle that should yield substantial accuracy, especially for small angles. A particular such configuration has already been characterized [3]; a general numerical survey under varying domain parameters is in preparation. In a work by Finn and Fischer, also in preparation, domains are characterized that yield a continuum of Γ as above, but corresponding to a contact angle $\gamma \neq 0$.

(iv) *The rectangle.* We denote the lengths of the sides by $2a$, $2b$, $a \geq b$. We find

$$R_\gamma = \frac{ab}{(a+b)\cos\gamma} < \frac{b}{\cos\gamma}. \tag{3}$$

Were an extremal arc to join two opposite sides as in Fig. 7, we would find $R_\gamma = b/\cos\gamma$, contradicting (3). Thus, in view of the theorem, it suffices to consider only arcs that join adjacent sides. One sees immediately that such an arc can be found if and only if $\gamma < \pi/4$, and a calculation shows that $\Phi < 0$ for every such configuration. (The arcs all have the same center, as indicated in Fig. 8.) It follows that *regardless of the aspect ratio b/a, a solution exists in a rectangle if and only if $\gamma \geq \pi/4$.*

The Rounded Rectangle

In this section we carry out in detail a new application of the basic theorem to a container whose section is a rectangle with sides of length $2a$, $2b$, $a \geq b$ that has been modified by rounding the corners with circular arcs of radius ϵ, see Fig. 9. Again, for simplicity, we restrict ourselves to wetting liquids, $0 \leq \gamma < \pi/4$. The results presented here show the effect of rounding on the value of the critical contact angle $\pi/4$ for the rectangle with sharp corners (Item (iv) in the above section). It is of importance to know this effect in practice, as corners fabricated from solid material often are rounded, not perfectly sharp.

We proceed as follows (application to other geometries would proceed similarly):

(i) *Calculation of* $|\Sigma|$, $|\Omega|$, *and* R_γ . The area $|\Omega|$ and perimeter $|\Sigma|$ of the cross-section

depicted in Fig. 9 are

$$|\Omega| = 4ab - (4 - \pi)\epsilon^2$$

and

$$|\Sigma| = 4(a + b) - 2(4 - \pi)\epsilon.$$

From these and (1) we find that the radius of any extremal arc Γ for contact angle γ is

$$R_\gamma = \frac{ab - (1 - \pi/4)\epsilon^2}{[a + b - 2(1 - \pi/4)\epsilon]\cos\gamma}. \tag{4}$$

(ii) *Placement of* Γ. The next task is to determine all possible ways of placing extremal arcs into Ω. This is generally the most difficult step. We commence with the result of the last section, that if $\epsilon = 0$, then extremals appear only if $\gamma < \pi/4$ and always join adjacent sides, yielding negative values for Φ (see Fig. 8). A similar behavior can be expected as rounding is introduced, and indeed a calculation shows that such extremals joining adjacent sides can still be found when γ is in the range

$$0 \le \gamma < \cos^{-1}\left(\frac{\epsilon}{2R} + \frac{\sqrt{2 - (\epsilon/R)^2}}{2}\right) \equiv \gamma_M.$$

The maximal angle γ_M occurs when the arc passes through the intersection of the circular and straight portions of the boundary. We thus seek extremals Γ for contact angle $0 \le \gamma \le \gamma_M$ that intersect the straight portions of the boundary, configured as in Fig. 10. (It suffices to consider one of the corners, as the same result is obtained in each.) Other extremal placements are considered in the next section, where it is shown they can be excluded.

(iii) *Calculation of parameter values for which* $\Phi = 0$. We next calculate Φ for the rounded rectangle (Fig. 9), with Γ placed as in Fig. 10. First, we find the area $|\Omega^*|$ bounded by the rounded corner region and an extremal arc Γ. One finds by a straightforward calculation that

$$|\Omega^*| = R_\gamma^2(\cos\gamma - \sin\gamma)\cos\gamma - (\pi/4 - \gamma)R_\gamma^2 - (1 - \pi/4)\epsilon^2.$$

Similarly, one finds that the length of the part of the boundary Σ bordering Ω^* is

$$|\Sigma^*| = 2[(\cos\gamma - \sin\gamma)R_\gamma - (1 - \pi/4)\epsilon]$$

and that the length of Γ is

$$|\Gamma| = 2(\pi/4 - \gamma)R_\gamma.$$

Substitution into (2) yields

$$\Phi = (\pi/4 - \gamma)R_\gamma - [(\cos\gamma - \sin\gamma)R_\gamma - 2(1 - \pi/4)\epsilon]\cos\gamma - (1 - \pi/4)\frac{\epsilon^2}{R_\gamma}. \qquad (5)$$

Two particular limiting cases have a special interest. One of these is the case $\gamma = 0$. The equation $\Phi = 0$ then simplifies to

$$\Phi = -\frac{1}{R_0}(1 - \pi/4)(R_0 - \epsilon)^2 = 0$$

which implies $R_0 = \epsilon$; that is, the extremal must coincide with the rounding arc. We place this result into (4) to obtain the quadratic equation for ϵ

$$(1 - \pi/4)\epsilon^2 - (a + b)\epsilon + ab = 0,$$

an equation with two real roots. Only one of these (with $\epsilon \leq b$) has physical meaning and corresponds to an extremal arc as depicted in Fig. 10. We find

$$\epsilon = \frac{a + b - \sqrt{(a + b)^2 - (4 - \pi)ab}}{2(1 - \pi/4)}. \qquad (6)$$

Numerical evaluation yields that ϵ increases from approximately $0.53b$ to b as a increases from b to infinity.

Another important limiting case is obtained by letting $a \to \infty$, for general γ. In the limit, one obtains from (4)

$$R_\gamma = \frac{b}{\cos\gamma},$$

independent of the rounding radius ϵ. We are led again to a quadratic, for which the physical root is

$$\epsilon = b - \frac{b}{2\cos\gamma}\sqrt{\frac{\pi - 4\gamma - \pi\cos^2\gamma + 4\sin\gamma\cos\gamma}{1 - \pi/4}}. \tag{7}$$

This yields the rightmost curve plotted in Fig. 11. (It has not yet been clarified mathematically whether a solution actually exists in this limiting case.)

In general, the equation $\Phi = 0$ yields a quartic in ϵ. But also in that case, only one of the roots (corresponding to (6) and (7) above) has physical meaning. To see that, we note again the general result [3] that at $\gamma = \gamma_{cr}$ there is at least one non-null extremal Γ in Ω, for which $\Phi = 0$. In the next section it will be shown that the only possible such configuration is the one just considered, as indicated in Fig. 10. As is shown in [8, p. 144], to each ϵ in the physical range there is a unique γ_{cr} determined by the configuration; these values yield the curves in Fig. 11. From the evident monotonicity of the curves, it follows that to each γ_{cr} (for given aspect ratio) there corresponds a unique ϵ, and we see that *three of the four roots of the equation* $\Phi = 0$ *must be superfluous.*

The curves in Fig. 11 depict the locus of physical points (ϵ, γ) for which $\Phi = 0$, for cross sections with various aspect ratios, as computed numerically from (4) and (5). From left to right, the curves are for aspect ratio $b/a = 1, 0.9, 0.8, \ldots, 0.1, 0$. Each curve gives the critical value of γ as a function of the nondimensional rounding radius ϵ/b. The intercept of each curve on the ϵ/b axis is the value determined by (6). For points below any given curve, Φ becomes negative and no solution exists. Above the curve, Φ is necessarily positive and a solution surface (unique for prescribed volume) is present. For points on the curves it can be shown for this example that solutions do not exist if $\gamma \neq 0$, but they do exist when $\gamma = 0$.

The behavior of the corresponding extremal arcs Γ can be summarized as follows. For $\epsilon = 0$, the behavior as γ increases is as indicated in Fig. 8: As γ increases from 0 to its critical value of $\pi/4$, R_γ increases from $ab/(a+b)$ to $\sqrt{2}ab/(a+b)$, and Γ moves to the corner. Similarly, for ϵ equal to a positive fixed value below one of the curves in

Fig. 11, as Γ increases from 0 to its critical value on the curve, R_γ increases and Γ moves toward the rounding arc, continuing to intersect the straight portion of the boundary, as indicated in Fig. 9. Now consider γ to be fixed at a value in the range $0 \leq \gamma < \pi/4$. As ϵ increases from zero to the critical value ϵ_γ on one of the curves in Fig. 11, R_γ increases from $ab/[(a+b)\cos\gamma]$ to ϵ_γ, and Γ moves away from the rounding arc (and continues to intersect the straight portion of the boundary, as in Fig. 9). Correspondingly, Φ achieves its smallest value (negative) at $\epsilon = 0$, $\gamma = 0$ and increases monotonically to zero as ϵ and γ increase toward a point on a curve in Fig. 11.

By reflecting the graphs in Fig. 11 upward about $\gamma = 90°$, one obtains an extension of the results to include nonwetting liquids ($90° < \gamma \leq 180°$); the region of nonexistence for the nonwetting liquids would then be in the upper left corner (i.e., $135° < \gamma \leq 180°$, and the same values of ϵ as for wetting liquids).

Exclusion of nonminimizing extremals for the rounded rectangle

In order to complete the reasoning for the rounded rectangle, it is necessary to show that when $\gamma = \gamma_{\rm cr}$ no configuration with $\Phi = 0$ can occur other than as indicated in the preceding section; specifically, we must show that $\Phi > 0$ for any other extremal arc Γ.

In what ways can extremal configurations appear? We first note that any such configuration yielding $\Phi = 0$ must minimize Φ, since at $\gamma = \gamma_{\rm cr}$, $\Phi < 0$ is not possible. By a result of Finn and Fischer [9], a non-null extremal Γ that meets two points of a single rounding arc cannot minimize, thus this possibility is excluded. Also, no extremal can meet Σ in one point of such an arc and in a point of an adjacent straight segment, as the intersection angles could not then both be γ.

We observe next that for the rounded rectangle configuration (Fig. 9), there holds

$$\frac{\Omega}{\Sigma} = \frac{ab - (1-\pi/4)\epsilon^2}{a+b-2(1-\pi/4)\epsilon}.$$

If $\epsilon = 0$, then $\frac{\Omega}{\Sigma} = \frac{ab}{a+b} < b$ (for $b \leq a < \infty$). For $0 < \epsilon < b$, the quadratic in ϵ obtained by

setting $\frac{\Omega}{\Sigma} = b$ has no real root, and therefore $\frac{\Omega}{\Sigma} < b$ for all ϵ in the physical range. Hence in that range $R_\gamma < b/\cos\gamma$, and it follows, as for the illustrative example of the rectangle with sharp corners (Fig. 7), that no extremal arc can meet two parallel linear segments of Σ .

Consider an extremal Γ that meets two diagonally opposite rounding arcs, as indicated in Fig. 12. Since Γ is minimizing, we conclude from Theorem 6.16 of [8] that $\delta + \gamma \leq \pi/2$. From that follows easily that the chord T joining the endpoints would have length $|T| \leq 2R_\gamma \cos\gamma$, so that the above bound on R_γ would yield $|T| < 2b$. But the shortest such segment is the one through the symmetry point of the rectangle and the centers of the rounding arcs, which has the length $2\sqrt{(a-\epsilon)^2 + (b-\epsilon)^2} + 2\epsilon > 2b$. Thus, this configuration cannot occur.

The only remaining possibility, other than that considered in the previous section, is indicated in Fig. 13 . Introducing a polar coordinate system with origin at the center of Γ and positive axis directed toward the arc of Γ indicated, we calculate the second variation $I[\eta]$ of Φ corresponding to the normal displacement $\eta = \cos\theta$ along the arc Γ; here θ is the polar angle measured from the bisector of the subtended angle 2α. That is, we translate Γ rigidly along its axis of symmetry. We obtain after a lengthy calculation

$$I[\eta] = -\sin 2\delta + \cos\gamma \cos^2\delta \left\{ 2 - (k_1 + k_2)\frac{R_\gamma}{\cos\gamma} \right\}.$$

Here k_1, k_2 are the curvatures of the boundary Σ at the two contact points, considered as positive when the curvature vector points into Ω. In the present case, $k_1 + k_2 > 0$ and $\delta + \gamma > \pi/2$, and we conclude immediately that $I[\eta] < 0$. It follows that Γ cannot be an arc of a minimizing configuration, and therefore that the corresponding Φ for any configuration in which Γ appears will be positive. We may therefore exclude also such arcs from consideration, and we are reduced to the configurations of Fig. 10.

Acknowledgment

We wish to thank M. Weislogel for bringing the rounded rectangle geometry to our attention.

References

[1] Albright, N., *Some properties of capillary surfaces on elliptical domains*, Report LBL-6137, Lawrence Berkeley Lab., Univ. of California, 1977.

[2] Concus, P., and R. Finn, *On capillary free surfaces in the absence of gravity*, Acta Math. **132** (1974), pp. 177–198.

[3] Concus, P., and R. Finn, *Continuous and discontinuous disappearance of capillary surfaces*, in Variational Methods for Free Surface Interfaces, P. Concus and R. Finn, eds., Springer-Verlag, New York, 1987, pp. 197–204.

[4] Concus, P., and R. Finn, *Capillary surfaces in microgravity*, in Low-Gravity Fluid Dynamics and Transport Phenomena, J. L. Koster and R. L. Sani, eds., AIAA, Washington, D. C., 1990 (to appear).

[5] Concus, P., R. Finn, J. M. Harris, and M. Mori, *Zero-g liquid reorientation in a bathtub-shaped cylinder*, (in preparation).

[6] Finn, R., *Existence criteria for capillary free surfaces without gravity*, Indiana Univ. Math. J. **32** (1983), pp. 439–460.

[7] Finn, R., *A subsidiary variational problem and existence criteria for capillary surfaces.* J. Reine Angew. Math. **353** (1984), pp. 196–214.

[8] Finn, R., *Equilibrium Capillary Surfaces*, Springer-Verlag, New York, 1986.

[9] Finn, R., and B. Fischer, *On the determination of critical contact angle*, (in preparation).

[10] Smedley, G., *Preliminary drop-tower experiments on liquid-interface geometry in partially filled containers at zero gravity*, Experiments in Fluids **8** (1990), pp. 312–318.

[11] Smedley, G., *Containments for liquids in zero gravity*, Applied Microgravity Tech. , (1990), (to appear).

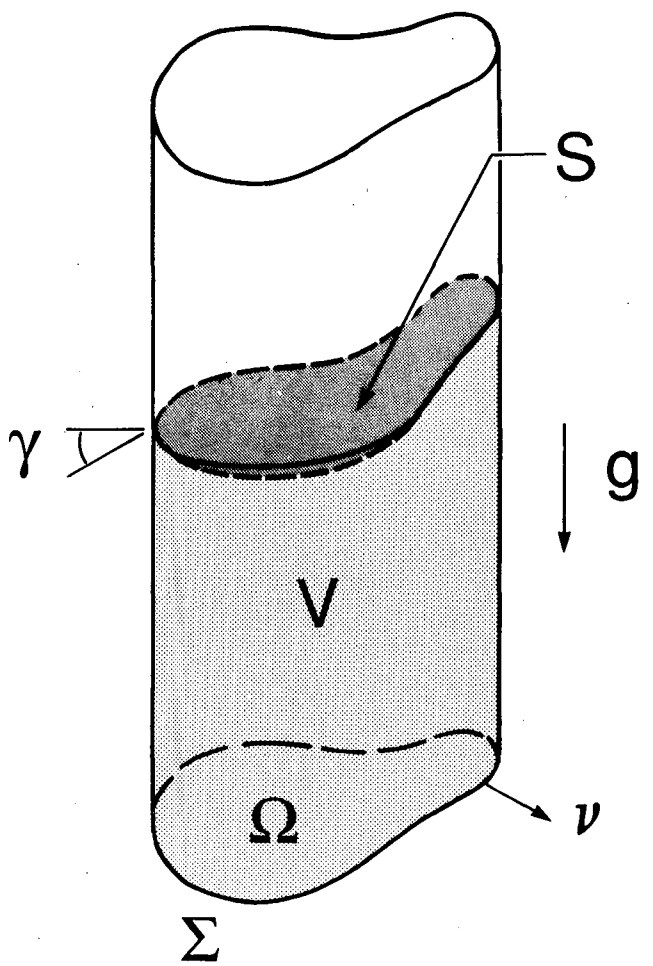

Figure 1. Partly filled cylindrical tube with base Ω.

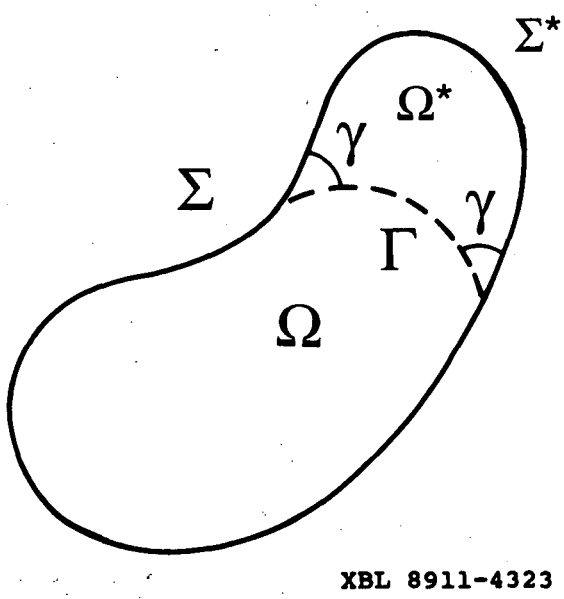

Figure 2. Domain partitioned by circular arc Γ of radius R_γ.

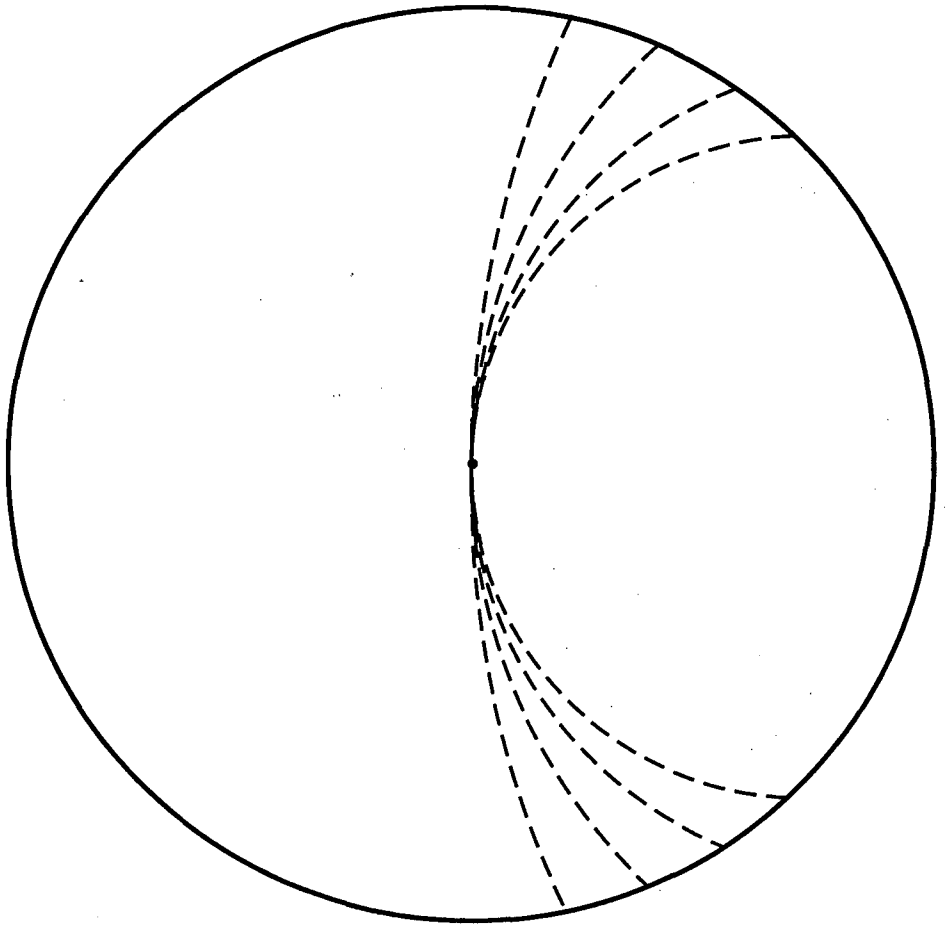

Figure 3. Extremal arcs for a circular tube; all arcs pass through the circle's center.

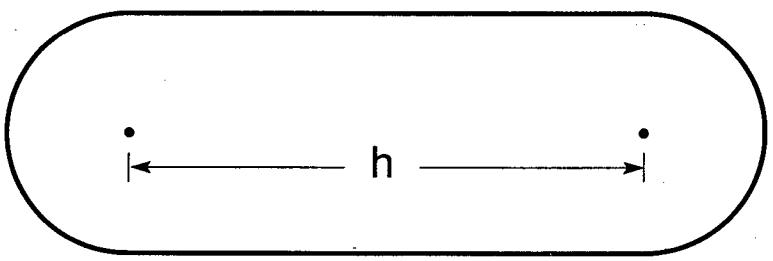

Figure 4. Section with parallel sides and circular arc ends.

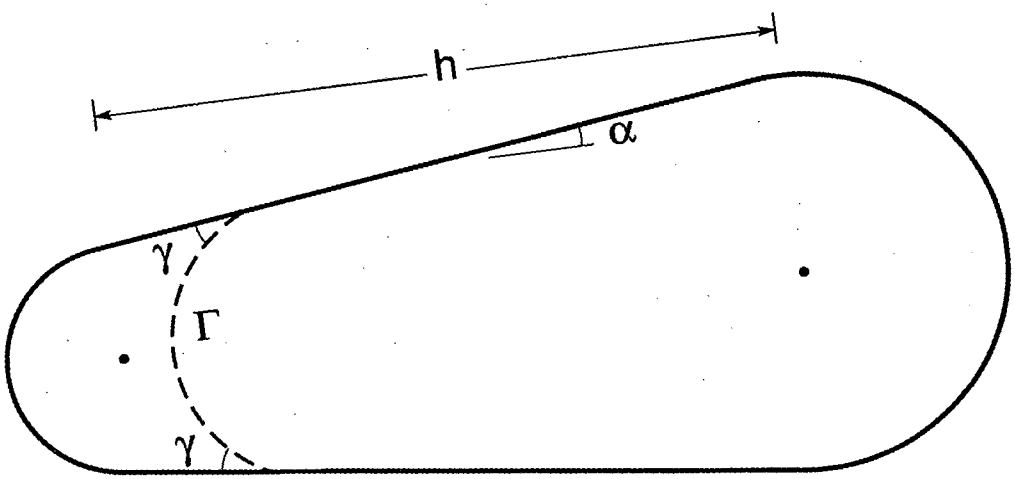

Figure 5. Section with non-parallel sides and circular arc ends.

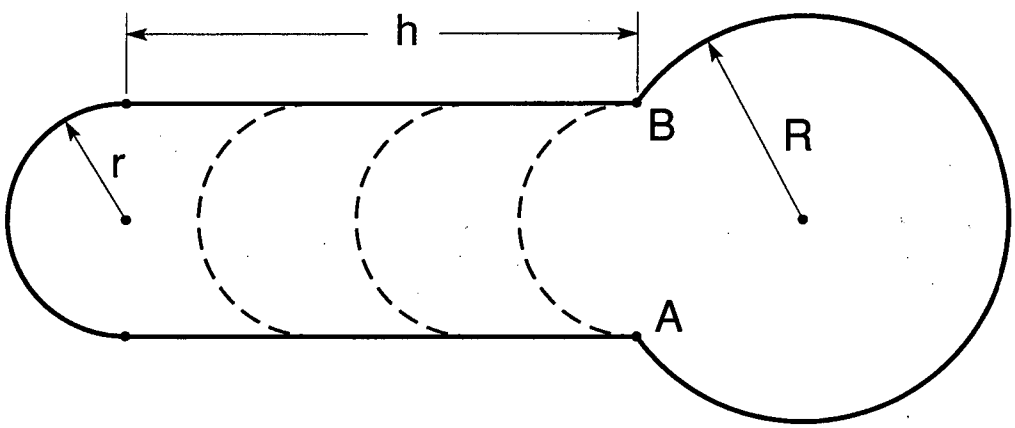

Figure 6. Keyhole section.

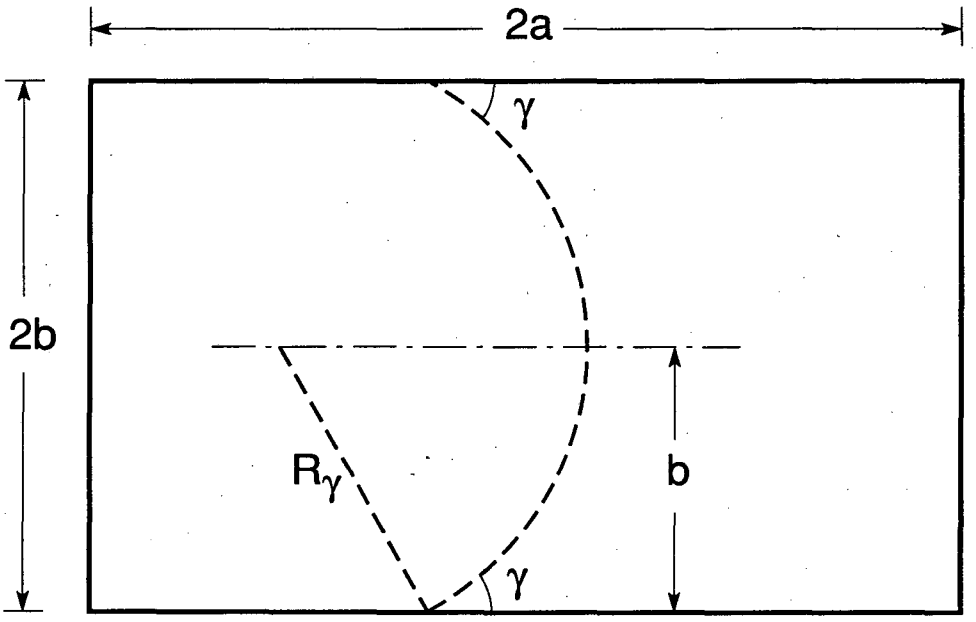

Figure 7. Excludable configuration for rectangular section.

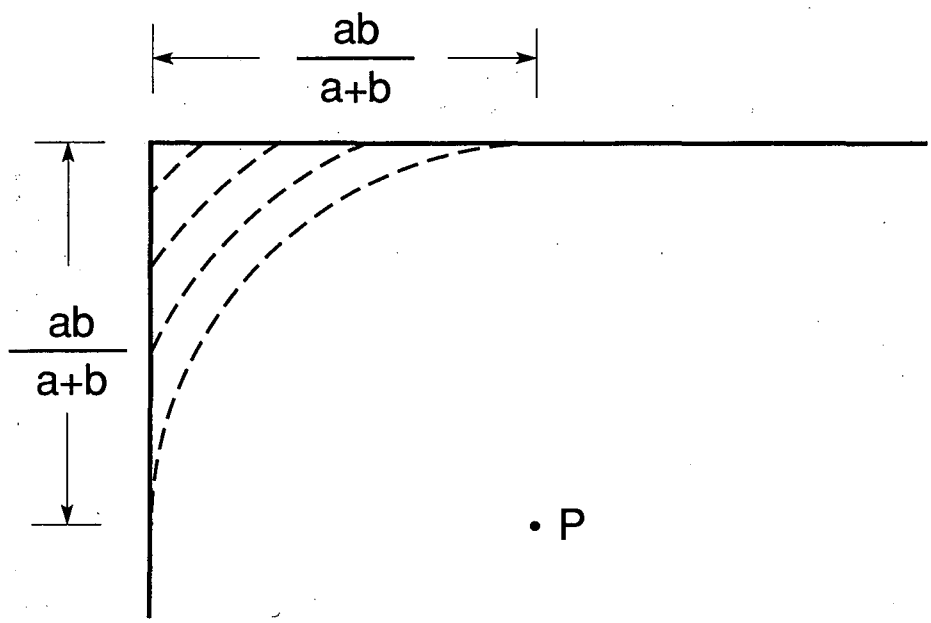

Figure 8. Extremal arcs for rectangular section; all arcs have the same center P.

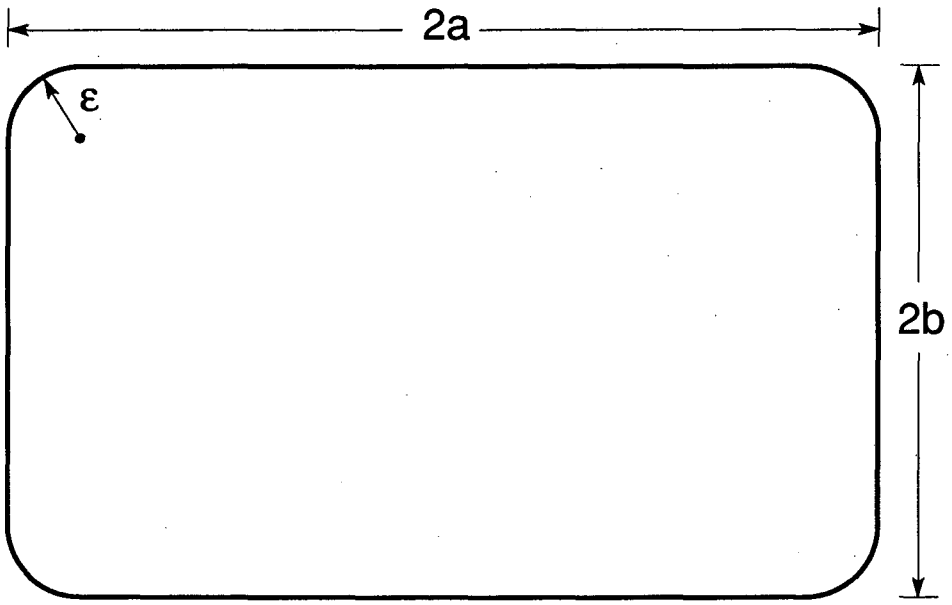

Figure 9. Rounded rectangle.

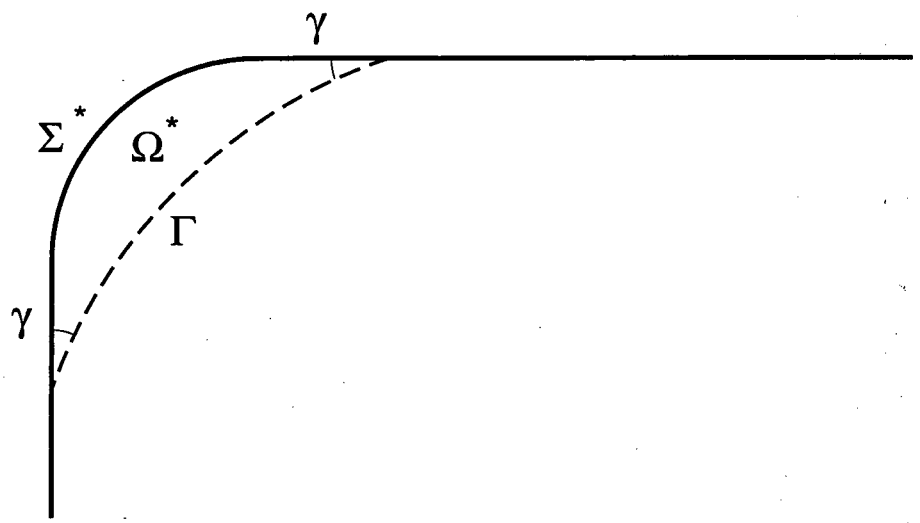

Figure 10. Extremal arc configuration for rounded rectangle.

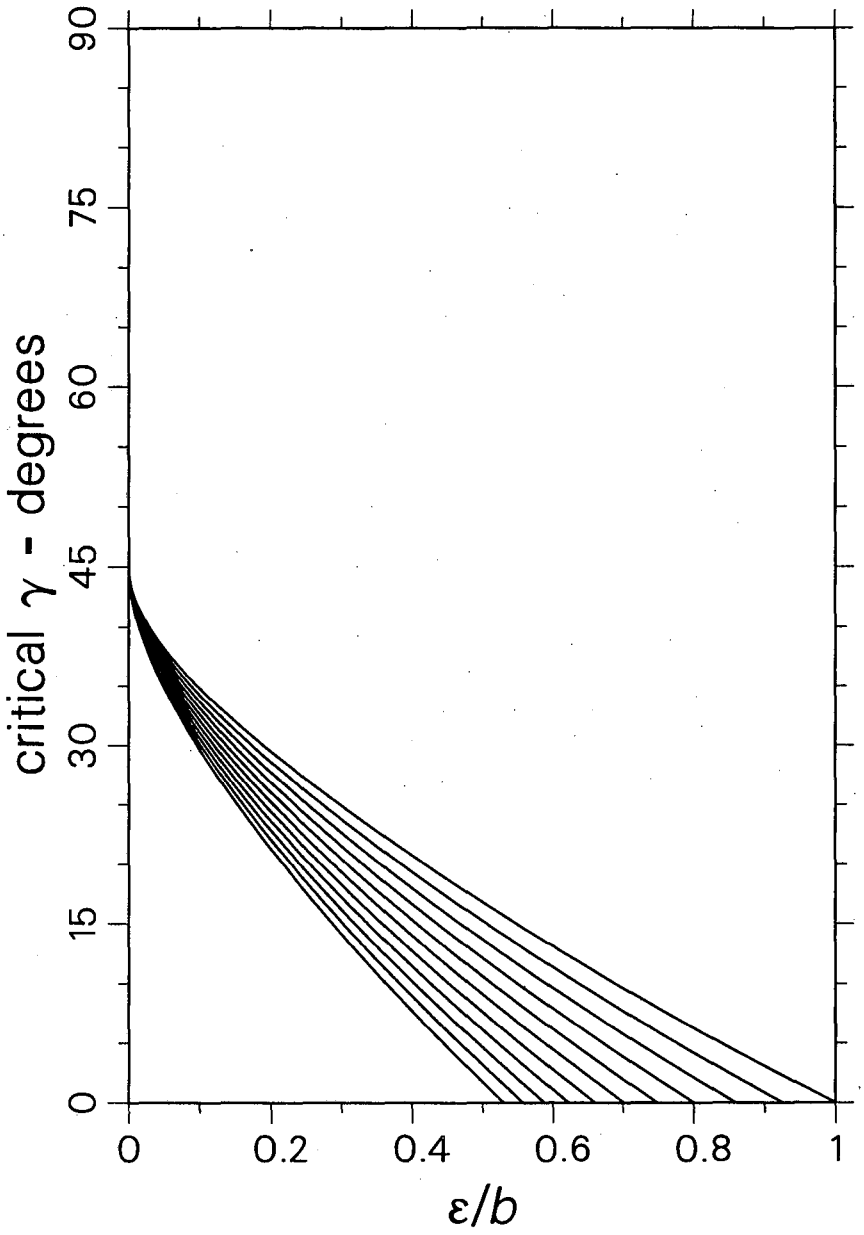

Figure 11. Critical contact angle vs. normalized rounding radius ϵ/b. Curves are for aspect ratio $b/a = 1, 0.9, 0.8, \ldots, 0.1, 0$, from left to right.

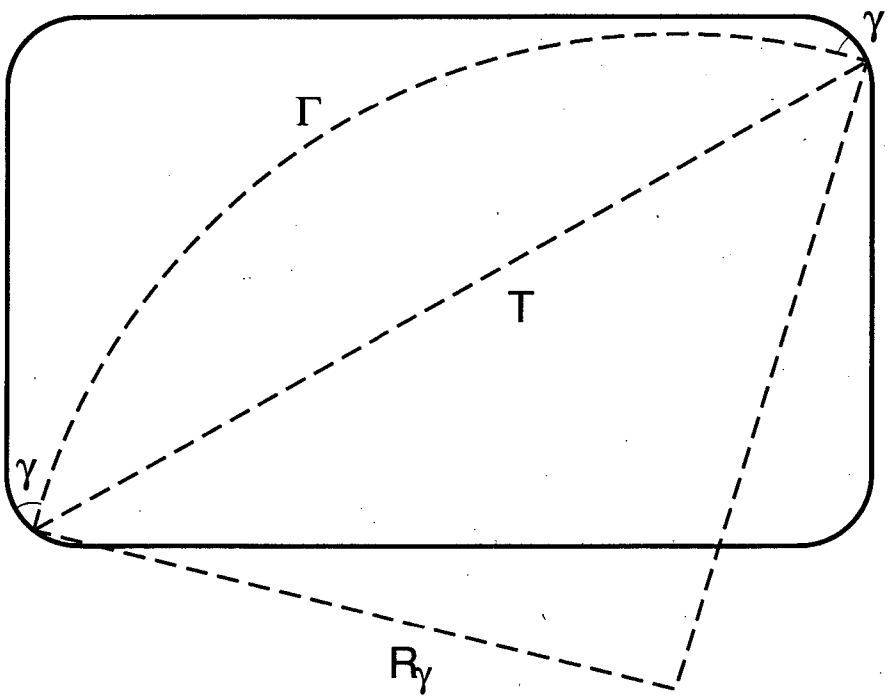

Figure 12. Excludable extremal.

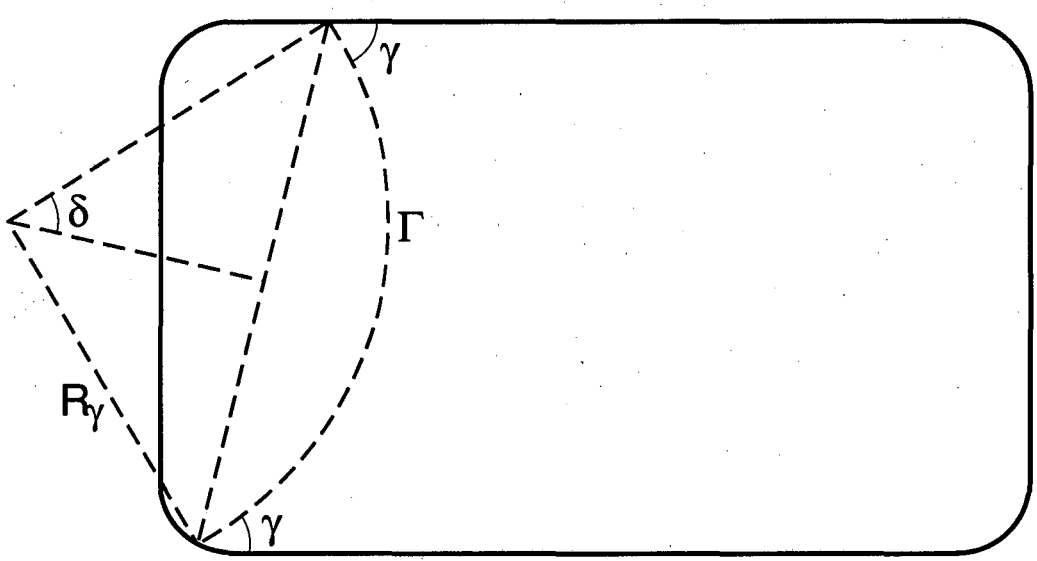

Figure 13. Excludable extremal.

LAWRENCE BERKELEY LABORATORY
UNIVERSITY OF CALIFORNIA
INFORMATION RESOURCES DEPARTMENT
BERKELEY, CALIFORNIA 94720